Array-measurements at the broadband-site “BOURR”

G. Stamm, J. Burjanek, D. Fäh

Location	Bourrignon (JU)
Seismic Station	BOURR
Method(s)	H/V-measurements Array-measurements
Date	BOURR1: 29.09.2008 BOURR2: 24.10.2008
Measurements done by	Gabriela Stamm
Processing done by	Gabriela Stamm, Jan Burjanek

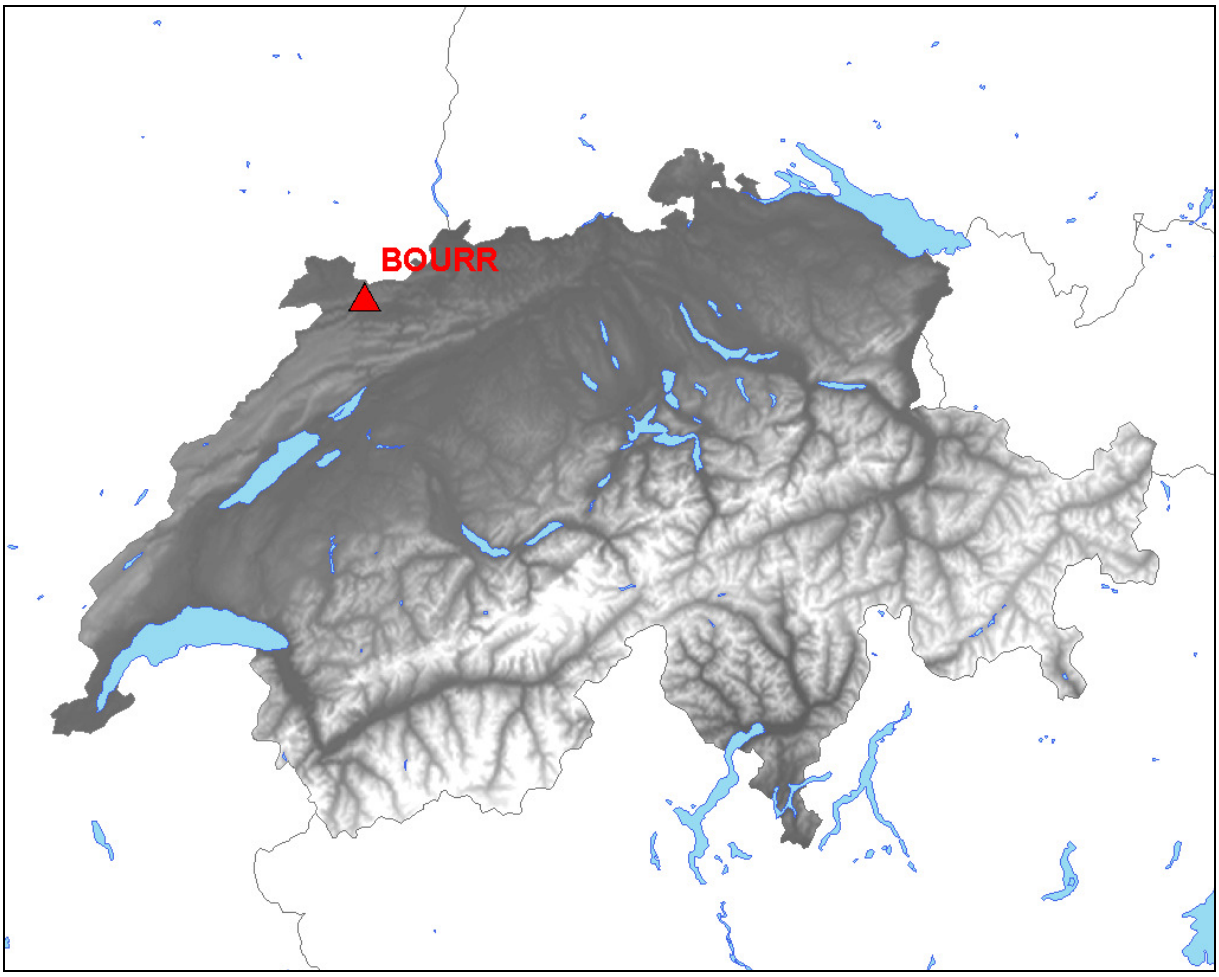

Figure1: *Location of the broadband-site BOURR in Bourrignon (JU).*

1. Method

H/V

To be sure that the measuring site can be handled as a “1D-case”, the H/V-ratios of all array-points were compared together. All Points showing differing curves were then excluded of the array-processing. To compute the H/V-ratios, two different methods were applied. The first one is the classical polarization analysis in the frequency domain, where the polarization is defined as the ratio between the quadratic mean of the Fourier spectra of the horizontal components and the spectrum of the vertical component. The second method tries to reduce the SH-wave influence by identifying P-SV-wavelets from the signal and taking the spectral ratio only from these wavelets. This is done by means of a frequency-time analysis of each of the three components of the ambient vibrations. Both methods are described in more detail in Fäh et al., 2001.

Array-processing

The array method we use is based on the high-resolution beam-forming (HRBF). It was originally proposed by Capon (1969) but developed and applied to vertical recordings of ambient vibrations by Kind et al. (2005). We have extended this method to analyse also the horizontal components (Fäh et al., 2008).
In general, sub-arrays with different apertures are set up for the measurement to optimise the capabilities in a certain frequency band. Small apertures are used to resolve the shallow part of a structure, and by increasing the aperture, deeper and deeper structures can be investigated. The finale dispersion curve over a wide frequency-range is then composed of the parts obtained by the different sub-arrays. The limits of each sub-array are given by the aliasing at high frequencies and the loss of resolution at low frequencies.

Inversion

Our inversion scheme is based on a genetic algorithm that was developed by D. Carroll and is described in Fäh et al. (2001, 2003). It does not require explicit starting models but only the definition of parameter limits. To estimate the average S-wave velocity structure below our array, we use as input the combined H/V spectral ratios and phase velocity curves for Rayleigh- and Love-Waves.

2. Array-Configuration

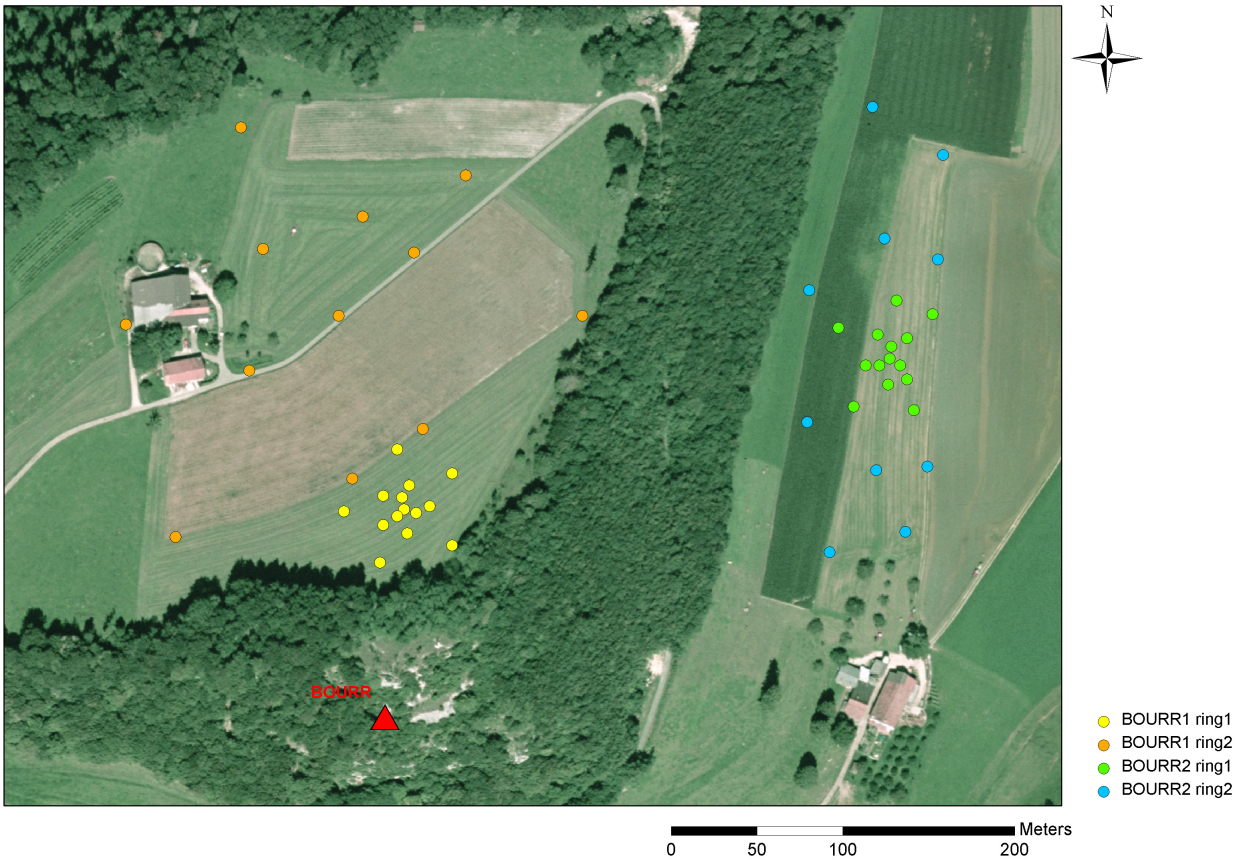

Figure 2: *Array-Configuration for BOURR1 and BOURR2.*

The site BOURR is located at a Jurassic hill range with two terraces. We set up two arrays, one on each terrace. The array BOURR1 is some tens of meters above the altitude of the broadband-station BOURR, the array BOURR2 is located at lower altitude.

Table 1: *important parameters of the array-setups.*

	BOURR1 ring1	BOURR1 ring2	BOURR2 ring1	BOURR2 ring2
# Sensors	14	13	14	11
max. Radius [m]	35	150	35	120
min. distance between two sensors [m]	7	60	7	65
max. distance between to sensors [m]	70	270	65	240

3. H/V

The comparison of the H/V-ratios of all stations from BOURR1 ring1 and ring2 show only one outlier in ring1. This station was then excluded from the array-processing. For BOURR2 ring2 we had to exclude four stations (the ones in green).

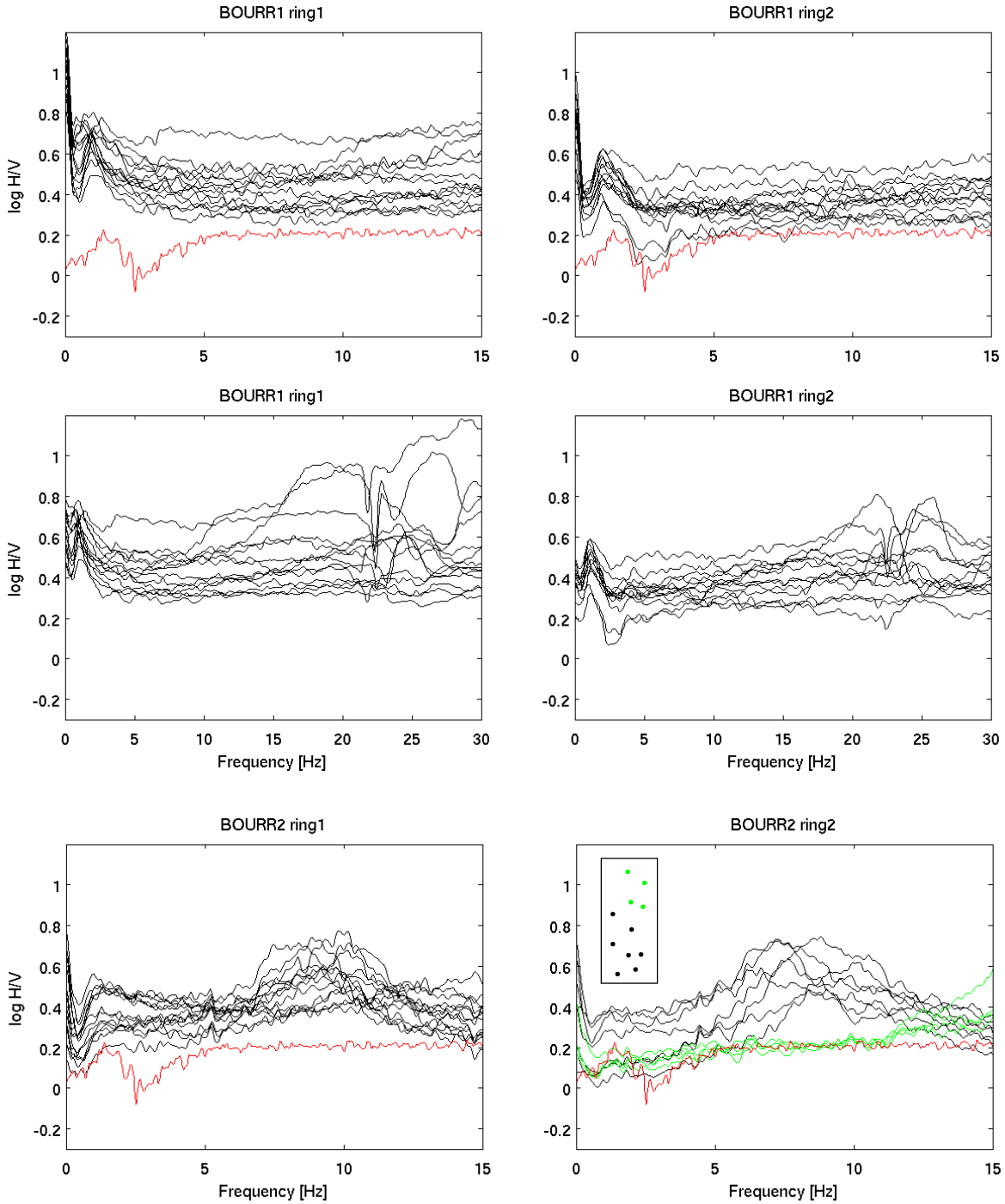

Figure 3: *Comparison of the H/V-ratios of all points measured in BOURR1 and BOURR2 (black) with the one from the broadband-station BOURR (red). For BOURR2 ring2 some points (northern part of the array) are plotted in green because they show a differing H/V-ratio.*

4. Dispersioncurves

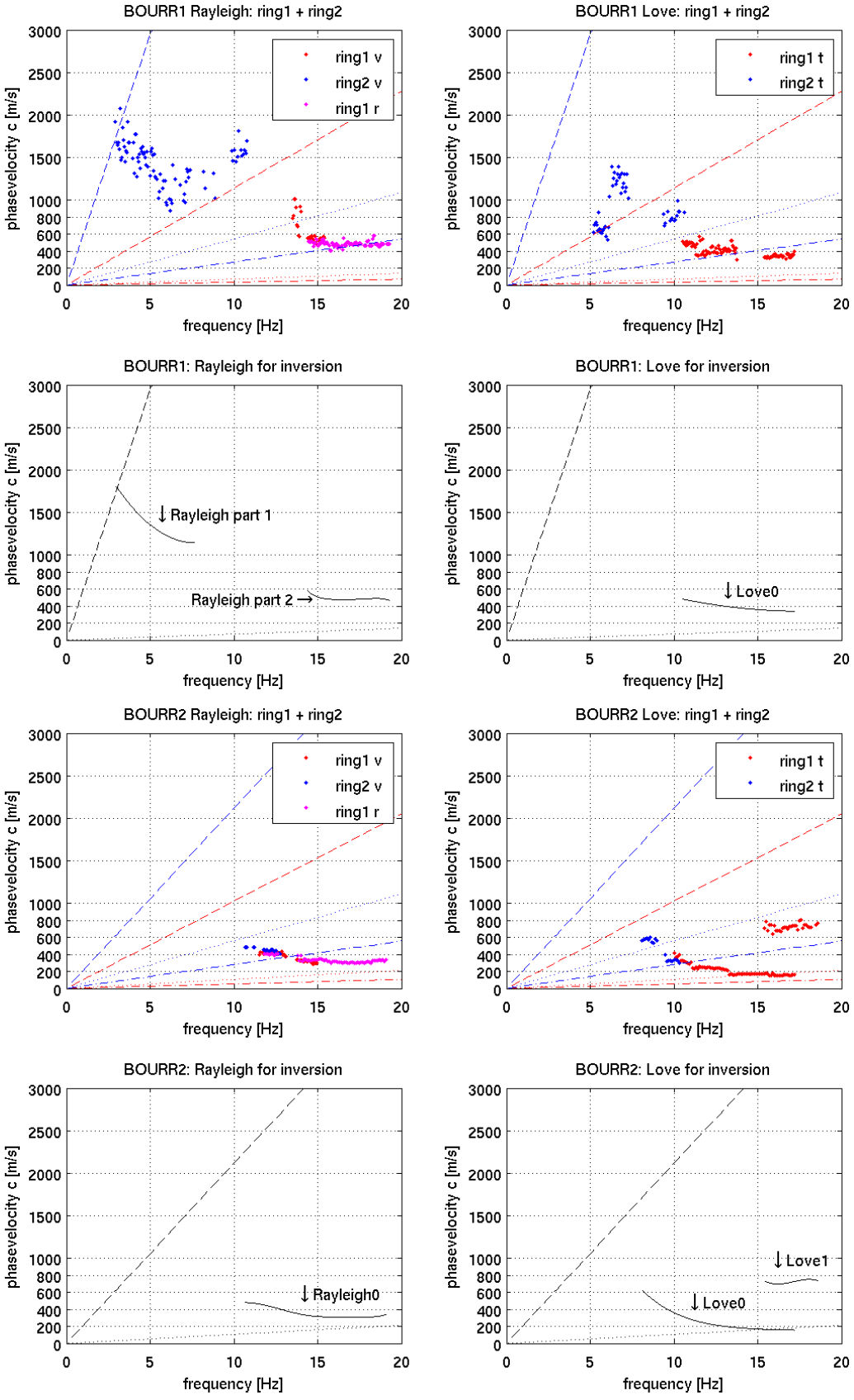

Figure 4: *Rayleigh- and Love-Dispersioncurves for BOURR1 and BOURR2. (v: vertical components, r: radial components, t: transverse components.)*

For BOURR1 the processing of ring1 provides parts of the fundamental modes of Rayleigh- and Love-waves for frequencies above 10Hz. On the vertical components of ring2 the picked points are quite scattered, but nevertheless we considered it either as a part of the first higher mode or as the fundamental mode of Rayleigh-waves.
For BOURR2, parts of the fundamental modes of Rayleigh- and Love-waves were clearly visible, and also a part of the first higher mode of Love-waves could be found.

5. Inverted Profiles

BOURR1:
Table 2 gives the description of three different types of models that were run for the site BOURR1. For all models, the Love wave dispersion curve between ~11-17Hz was fitted as part of the fundamental mode. The two parts of Rayleigh wave dispersion curve were once fitted both as fundamental mode (type 2), and then part 1 as fundamental mode and part 2 as first higher mode (type 3) and vice versa (type 1). Only for the type 1 models we tried to fit also the H/V curve between 1 and 1.9Hz. But because the fitting was quite bad we didn't made this for the two other types of models. The different assignments of Rayleigh modes take into account the large scatter of the picked phase velocities at low frequencies.
In Figure 5 the inverted S-wave profiles are shown. The different types of models for BOURR1 are given in different colour. The models of type 1 are printed in blue, type 2 in red and the ones of type 3 in green. The biggest differences between the different types are visible between a depth of 25m and 150m due to the assignment to a mode number and the loss of resolution below a certain depth.

Table 2:

	H/V	Rayleigh fund. mode	Rayleigh 1. higher mode	Love fund. mode
type 1	1-1.9Hz	14.5-18.5Hz	3.1-7.5Hz	11-17Hz
type 2	not fitted	3-8.5Hz and 14-19Hz	-	11-17Hz
type 3	not fitted	3.2-8Hz	14-19Hz	11-16.5Hz

BOURR2:
For the site BOURR2, only one type of models was inverted (see Table 3). After the experience we made with the inversion at site BOURR1 we didn't try to fit the H/V-curve for the site BOURR2 (the peak is also less clear at the site BOURR2). The picked parts of dispersion curves could be assigned to the fundamental or first higher mode. Due to the restricted information contained in the dispersion curves, and the measured low velocities, the measurements are not useful to characterize the site of the instrument (the station is in a bunker presumably in rock). The location of the array BOURR2 is on a site with very soft sediments (vs around 200 m/s). For BOURR2 only one type of models was inverted (see Figure 5).

Table 3:

	H/V	Rayleigh fund. mode	Love fund. Mode	Love 1. higher mode
Type 1	not fitted	11-17Hz	8.2-15.5Hz	16-18Hz

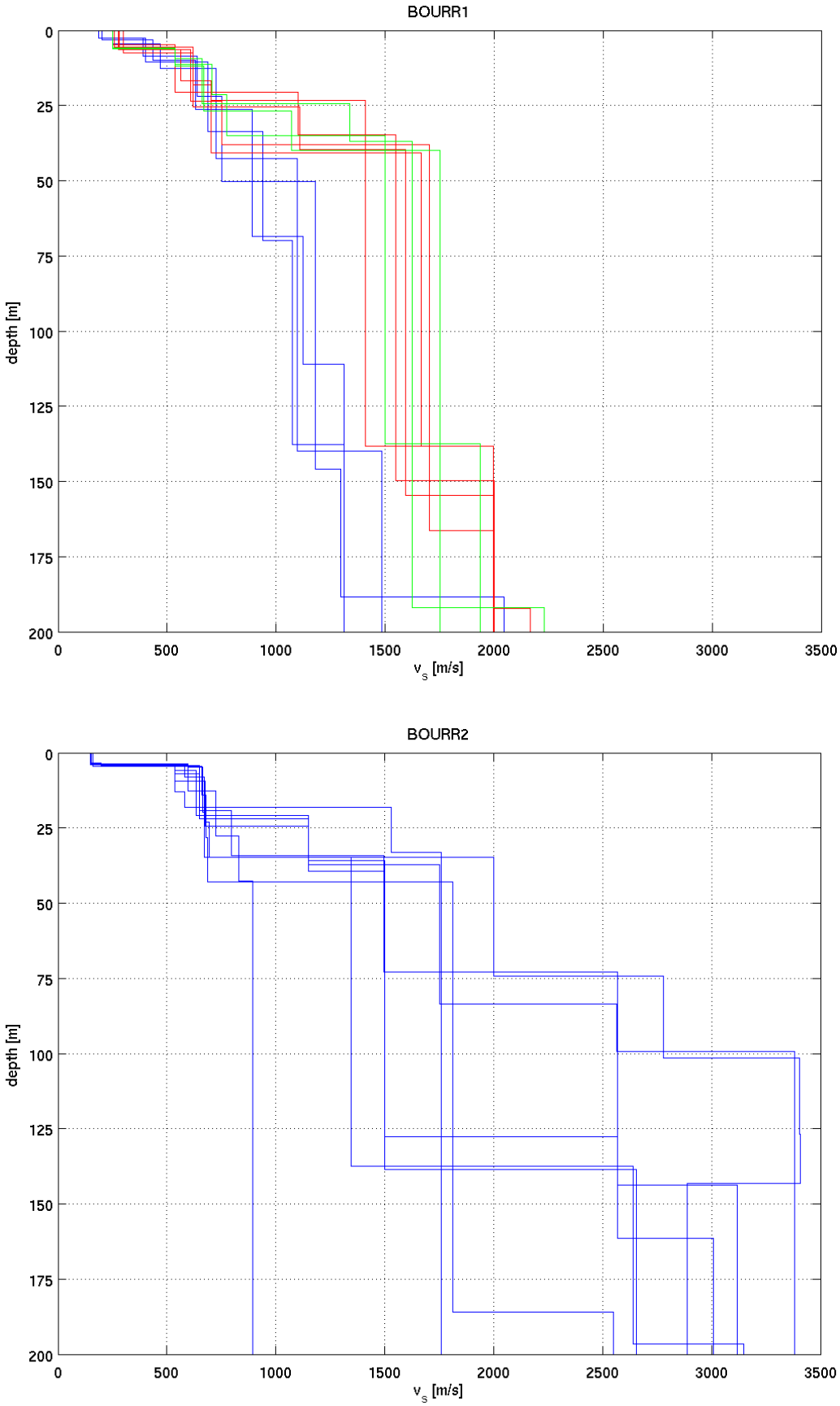

Figure 5: *Inverted S-wave profiles for the sites BOURR1 and BOURR2.*

Figures 6 and 7 show the fit of the theoretical dispersion curves of the inverted models to the observed dispersion curves for site BOURR1. The fit is generally good except for the type 3 models (green curves) and Love waves in Figure 7.

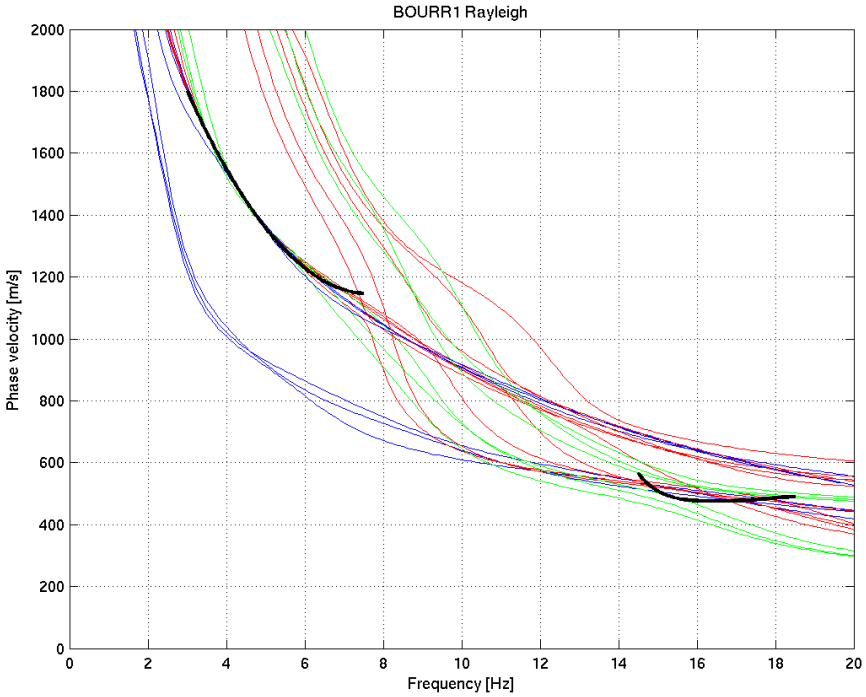

Figure 6: *Comparison between dispersion curves of the inverted structural models (black) and measured curves for Rayleigh waves (colour). The different types of models for BOURR1 are given in different colours according to Table 2. The fundamental and first higher modes are shown for all models.*

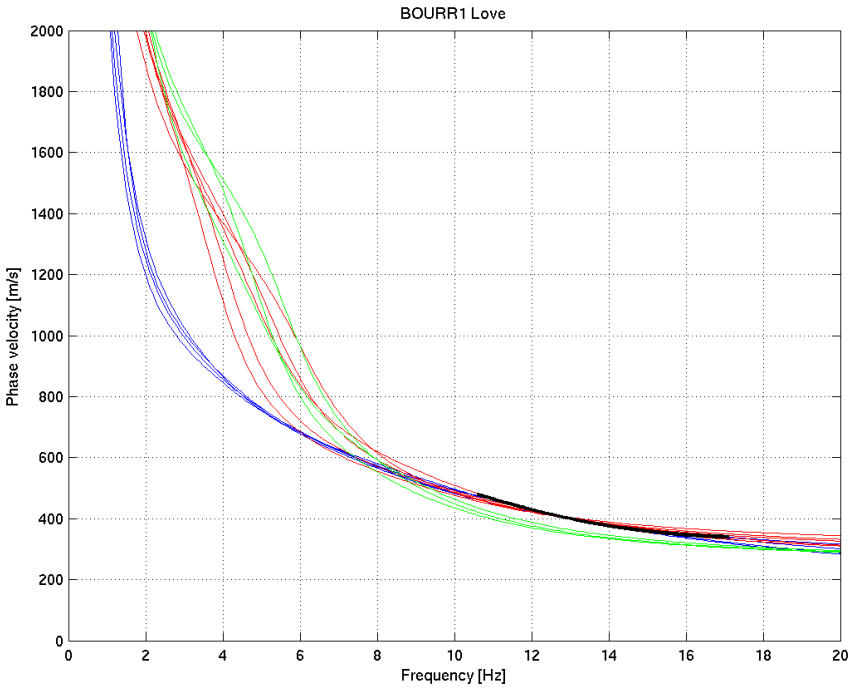

Figure 7: *Comparison between dispersion curves of the inverted structural models and measured curves for Love waves. The different types of models for BOURR1 are given in different colours according to Table 2. Only the fundamental mode is shown for each model.*

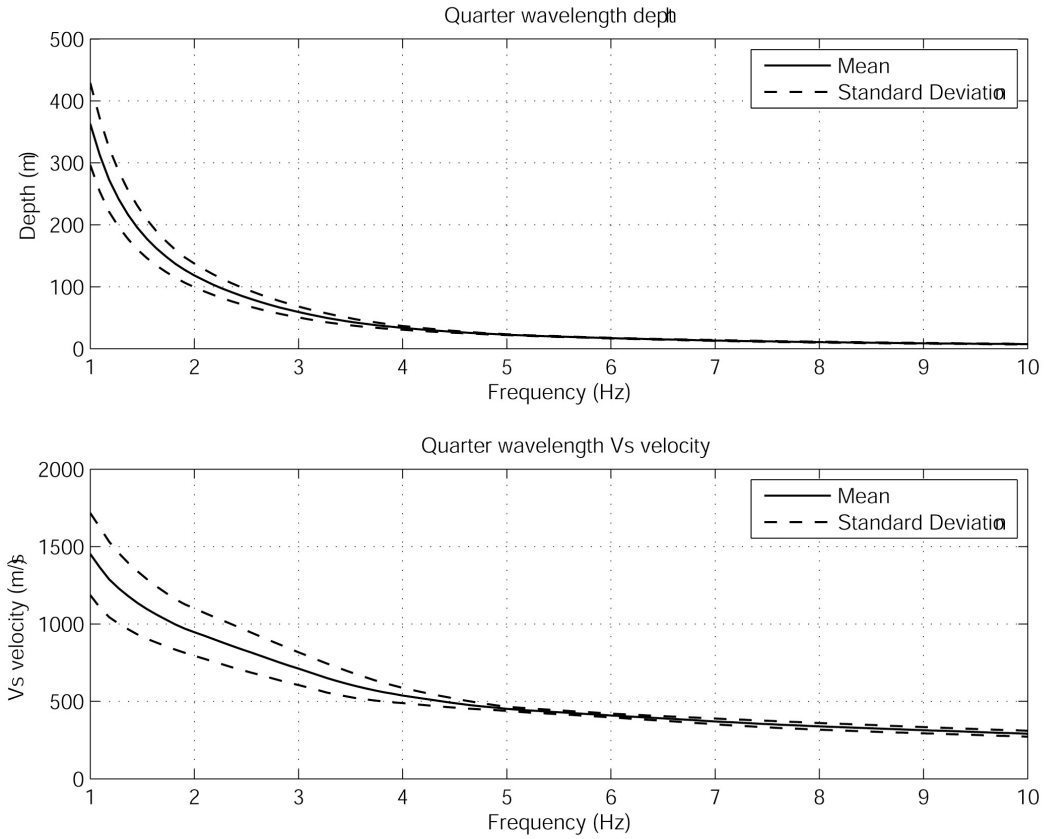

Figure 8: *Quarter wavelength and quarter-wavelength velocity as a function of frequency at the site of the arrays at BOURR1.*

Finally Figure 8 provides the quarter-wavelength velocities and depth as function of frequency for the ambient vibration array measurements. The seismic station BOURR1 is located in a bunker on rock. Table 4 summarizes the mean velocity for different thicknesses from the free surface of the upper terrace (Figure 2). The average velocity is computed in a way such that the travel-time in an average model corresponds to the sum of the travel times in the single layers:

$$\frac{1}{\bar{v}} = \frac{1}{H}\sum_{i=1}^{n}\frac{h_i}{v_i} \qquad \text{with} \qquad H = \sum_{i=1}^{n} h_i \,.$$

Table 4: *Mean S-wave velocity at BOURR1 over the thickness H.*

H [m]	Vs mean [m/s]	Vs stdev [m/s]
5	262	16
10	331	13
20	433	9
30	508	18
40	577	36
50	648	51
100	886	94
150	1022	118
200	1138	137

6. References

Capon, J., (1969). High-resolution frequency-wave number spectrum analysis, Proc. IEEE, 57(8), 1408-1418.

Fäh, D., Kind, F. and Giardini, D. (2001). A theoretical investigation of average H/V ratios. Geophys. J. Int., 145, 535-549.

Fäh, D., Kind, F. and Giardini, D., (2003). Inversion of local A-wave velocity structures from average H/V ratios, and their use for the estimation of site-effects, J. Seismol., 7, 449-467.

Fäh, D., Stamm, G. and Havenith, H.-B., (2008). Analysis of three-component ambient vibration array measurements, Geophys. J. Int., 172, 199-213.

Kind, F., Fäh, D. and Giardini, D., (2005). Array measurements of S-wave velocities from ambient vibrations, Geophys. J. Int., 160, 114-126.

Yamanaka, H., Takemura, M., Ishida, H. and Niea, M. (1994). Characteristics of long-period micro-tremors and their applicability in exploration of deep layers. Bull. Seism. Soc. Am., 84, 1831-1841